Strained interface layer contributions to the structural and electronic properties of epitaxial V_2O_3 films

Hamidreza Hajihoseini,[1,2] Einar B. Thorsteinsson,[1] Vilborg V. Sigurjonsdottir,[1] and Unnar B. Arnalds[1,*]

[1] *Science Institute, University of Iceland, Dunhaga 3, IS-107 Reykjavik, Iceland*
[2] *Industrial Focus Group XUV Optics, MESA+ Institute of Nanotechnology, University of Twente, 7522 NH Enschede, The Netherlands*

(Dated: March 29, 2021)

We report on the transport properties of epitaxial vanadium sesquioxide (V_2O_3) thin films with thicknesses in the range of 1 to 120 nm. Films with thickness down to nanometer values reveal clear resistivity curves with temperature illustrating that even at these thicknesses the films are above the percolation threshold and continuous over large distances. The results reveal that with reducing thickness the resistivity of the films increases sharply for thicknesses below 4 nm and the metal-insulator transition (MIT) is quenched. We attribute this increase to a strained interface layer of thickness $\sim$ 4 nm with in-plane lattice parameters corresponding to the Al_2O_3 substrate. The interface layer displays a suppressed MIT shifted to higher temperatures and has a room temperature resistivity 6 orders of magnitude higher than the thicker V_2O_3 films.

Vanadium sesquioxide (V_2O_3) is known to exhibit a metal-insulator transition (MIT) as a function of temperature with a jump in the resistivity of several orders of magnitude. This transition was first observed by Foex in 1946 [1] and since then has been extensively observed and investigated [2, 3]. In thin film form, several aspects have been shown to affect the transport properties and MIT in V_2O_3. The temperature and magnitude of the MIT for films deposited on single crystal substrates, can be influenced with the choice of substrate [4], deposition methods and conditions [5] and tuned through direct application of strain [6, 7], hydrostatic pressure [8, 9] and doping [10]. Although a few reports on the effect of the thickness of V_2O_3 on its MIT behavior have been published previously, they have been limited in number and scope and there are significant controversies in the literature on the results. V_2O_3 thin films deposited using reactive thermal evaporation on *c*-plane sapphire substrates have been shown to undergo a metal-to-semiconductor transition as their thickness decreases from 20 to 5 nm [11]. Films grown on annealed *c*-plane sapphire have been shown to have a different thickness dependence as compared to films grown on un-annealed sapphire [12]. Allimi et al. [13] reported on the change from insulator-insulator to metal-insulator, and then metal-metal transitions as the thickness of V_2O_3 increased from 12 to 46 nm.

In the present study, we investigate V_2O_3 thin films with thickness in the range of 1 to 120 nm grown on [0001] oriented Al_2O_3 substrates. Combining electrical measurements and structural investigations on the films using x-ray diffraction we are able to correlate changes in the resistivity of the films to a strained interface layer created during the initial stages of the film growth. The interface layer has an in-plane *a* lattice parameters corresponding to the underlying Al_2O_3 and an out-of-plane *c* lattice parameter slightly above bulk values for V_2O_3. Combined these parameters result in a c/a ratio substantially higher than for bulk V_2O_3. Our findings show that the fully strained interface layer stabilizes the insulating state with films of reducing thickness transitioning towards higher room temperature resistivity and a suppression of the MIT.

The V_2O_3 thin films were deposited by reactive dc-magnetron sputtering (dcMS) [14]. A mixture of 20 sccm argon and 1.5 sccm oxygen was injected into the sputtering chamber which resulted in a total growth pressure of 0.38 Pa. The substrates used were single side polished *c*-plane sapphire (Al_2O_3 (0001)). The substrates were annealed for 30 min at 600°C in vacuum prior to deposition. This temperature was maintained during growth as well. Before ex situ characterization, the samples were allowed to cool down in vacuum to room temperature. The micro-structural properties and the surface morphology of the V_2O_3 films were studied by x-ray diffraction (XRD), x-ray reflectivity (XRR), reciprocal space mapping (RSM), and atomic force microscopy (AFM). The electrical resistivity of the films was measured as a function of temperature using a two point resistance measurement setup in the temperature range of 20 K to 300 K with a ramp rate of 1 K/min using a helium cooled cryostat in vacuum. For this purpose, gold electrodes were deposited using electron beam evaporation on two sides of the films in order to provide reliable electrical contacts to the films. Further details on the growth system and deposition and experimental techniques are given in supplementary material.

Figure 1 shows X-ray diffraction scans for different thicknesses in the series. All films show a clear V_2O_3 (0006) peak confirming the highly epitaxial nature of the films and Laue fringes extending from the peak towards both sides revealing that the coherence lengths of the films in the vertical direction are close to that of the film thicknesses. For the thicker films a higher peak position is observed while for films below 8 nm in thickness the

*uarnalds@hi.is

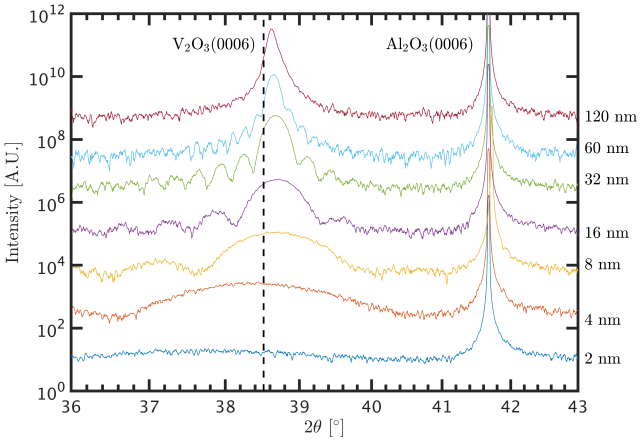

FIG. 1: X-ray diffraction scans for V_2O_3 films of varying thickness. The dashed line illustrates the angular (0006) peak position for bulk V_2O_3 [15]. Data for the 1 nm film did not have sufficient intensity to reveal any quantitative results on the V_2O_3 film.

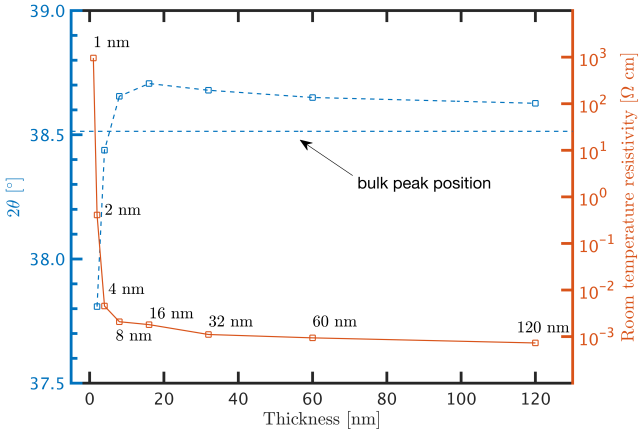

FIG. 2: Left axis: The (0006) XRD peak position of V_2O_3 plotted as a function of film thickness in the range 2 to 120 nm. The dashed lateral line illustrates the peak position for bulk V_2O_3. Right axis: Room temperature resistivity for all the films down to 1 nm thickness.

peak position is shifted to below bulk values indicating an increasing c lattice parameter with reduced thickness (see figure 2).

As the Al_2O_3 has a 4.1% smaller in-plane bulk lattice parameter than V_2O_3 a compressive in-plane strain is present in the V_2O_3 interface layer. Considering this in-plane compressive strain one would therefore expect a tensile strain in the out-of-plane c-lattice parameter. As can be seen in Fig. 2, the V_2O_3 (0006) peak for the thinner films shifts towards lower angles compared to bulk in agreement with an increased c-lattice parameter. However, as the films become thicker the films relax towards bulk values and for thicknesses of 16 nm and above a smaller c-lattice parameter is observed indicative of a compressive strain in the films.

Figure 3 shows RSM scans recorded around the (-1 0 -1 10) peaks for both V_2O_3 and Al_2O_3 in a glancing exit condition for the 4 nm and 16 nm thick V_2O_3 films. RSM scans for all the films are provided in supplementary material. In all cases the scans reveal a clear peak with a lateral a lattice parameter corresponding to the a lattice parameter of Al_2O_3 while having a vertical c-lattice parameter close to bulk value for V_2O_3. These results reveal the presence of a fully strained V_2O_3 layer at the interface. The thicker films show a second peak corresponding to a relaxed component of the films positioned close to bulk values. Films with thicknesses of 4 nm and below do not reveal any relaxed component indicating that the extent of the fully strained interface layer is around 4 nm.

The extent of the interface layer is additionally illustrated in the room temperature resistivity of the films as can be seen in Figure 2. For thicknesses below 4 nm the films reveal a sharp increase in the resistivity with decreasing thickness. No island growth was observed for these films from atomic force microscopy (see supplementary Fig. S1) indicating that the layering of the films is continuous and that the percolation threshold for the films is below 1 nm. These results therefore indicate that the fully strained interface layer has a substantially higher resistivity than bulk V_2O_3 (see supplementary Fig. S2).

Figure 4 shows the resistivity of all the films fabricated in this study as a function of temperature. The thickest films (120 and 60 nm) show a clear MIT shifted to lower values compared to bulk V_2O_3. As the thickness decreases the transition becomes more and more suppressed with a concomitant increase in the overall resistivity of the films. Films with thicknesses of and below 4 nm show a fully suppressed transition and a sharp order of magnitude overall increase in resistivity. These results are in direct contrast to results presented in ref. [4] where a suppression of the transitions is observed with a shift to lower temperatures with decreasing thickness. However, it should be noted that the samples presented in ref. [4] are grown by molecular beam epitaxy.

The choice of substrate plays a strong role in the observed MIT behavior. Considering the 4.1% smaller in-plane lattice parameter of Al_2O_3 compared to V_2O_3, large effects due to strain are expected, affecting the MIT. The results shown in Fig. 3 reveal the strain to be limited to a layer of finite thickness at the interface. Above this layer the V_2O_3 relaxes towards more bulk like lattice parameters, resulting in substantially less strain. Although the strained interface layer is limited to ~ 4 nm in thickness it has a profound effect on the MIT of films with substantially larger total thicknesses with a more normal MIT in the case of our films only being observed for the films with thicknesses of 60 nm or higher.

The relaxed V_2O_3 layer component preferentially re-

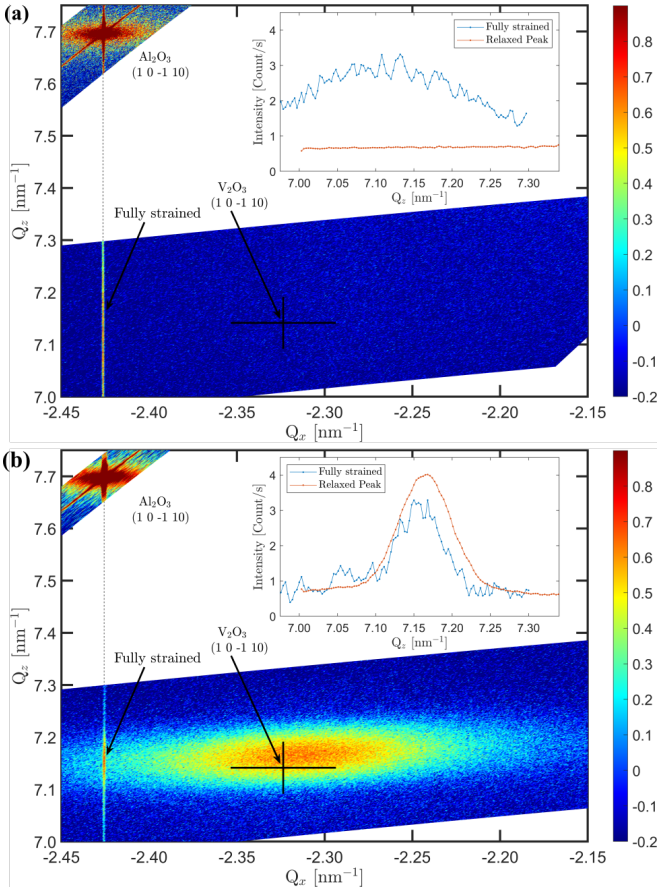

FIG. 3: Reciprocal space maps recorded for the (-1 0 -1 10) peak for the (a) 4 nm and (b) 16 nm thick films of V_2O_3. The same peak is recorded for Al_2O_3 for calibration purposes. The results reveal a clear peak for the V_2O_3 with Q_x values corresponding to Al_2O_3 revealing the presence of a fully strained interface layer. The 16 nm film additionally reveals a peak corresponding closely to the bulk value for V_2O_3 (illustrated with a black cross in the figures). The same peak is not observed for the 4 nm film indicating that only a fully strained component is present. The inset shows the linescans through the fully strained and relaxed peaks for the V_2O_3 film. The color coding is logarithmic and shifted to match the intensity of the V_2O_3 peaks and the Al_2O_3 is therefore saturated in the graph.

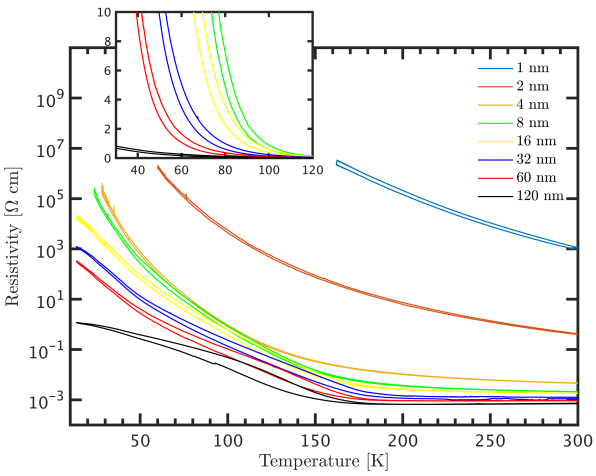

FIG. 4: Resistivity as a function of temperature for films with thicknesses in the range of 1 and 120 nm. As the film thickness decreases the resistivity curves transition towards higher values as the contribution from the fully strained V_2O_3 interface layer becomes larger. The inset depicts the resistivity on a linear scale for the films with thicknesses 16 nm and higher. All films were measured down to 20 K, however, resistivity measurements were in some cases limited by the minimum measurable current (10 pA).

veals a reduced c-lattice parameter and an increased a-lattice parameter (compared to bulk values). These results are in agreement with the thermal expansion of bulk V_2O_3 where a reduction in the c-lattice parameter with increasing temperature has been observed up to ~600°C while the a-lattice parameter becomes larger with increasing temperature. We have previously shown that the lattice parameters of V_2O_3 can be affected by interstitial oxygen which preferentially increases the a-lattice parameter for V_2O_3 [16, 17]. Combined these shifts in the a and c lattice parameters then result in a reduced c/a ratio compared to bulk. In bulk V_2O_3 the transition to the low temperature insulating state is accompanied by a reduction in c/a ratio [6] and in thin film form the resistance change from room temperature down to 50 K has been shown to increase with reduced c/a [18].

The growth mode of V_2O_3 on c-plane sapphire has been shown to favor island growth with an accompanying spherical growth which expands the in-plane lattice parameters of the surface layers [19]. Extracting the in-plane a lattice parameter of the films from the relaxed component in the RSM data we observe the similar trend of negative pressure (a larger than bulk value) for thicknesses above 4 nm. Graphs showing the a and c lattice parametar and the c/a ratio for both the relaxed and fully strained components of the films are shown in supplementary Fig. S4. As we have shown the growth of V_2O_3 on c-plane Al_2O_3 occurs with an initial fully strained layer with a subsequent relaxed layer forming on top. Figure 5 shows the mosaicity and lateral correlation length derived from the RSM scans (Supplementary Fig. S3). Initially the relaxed component has a substantial mosaicity which decreases rapidly as the film thickness increases with a concomitant increase in the lateral correlation length of the films. These results therefore reveal that the increased mosaicity of V_2O_3 films arises from the strain relaxation in the initial stages of the forming of a relaxed layer in opposition to the increased mosaicity of a spherical growth mode arising from later components in the growth [19]. As the film thickness increases further this mosaicity continues to decrease with a simultaneous increase in the grain size of the films.

For the fully strained interface layer the a-lattice parameter is substantially reduced ($a = 0.476$ nm) resulting in a substantially higher c/a ratio for the interface

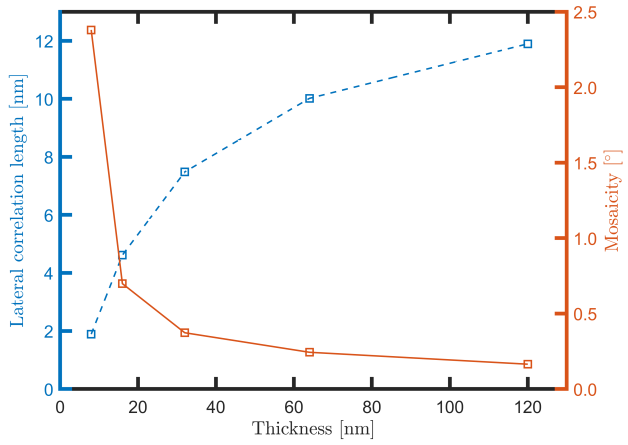

FIG. 5: The lateral correlation length (left axis, dashed line) and mosaicity (right axis, solid line) of the relaxed component of the films as a function of film thickness. The values were determined from fitting the relaxed component of the (-1 0 -1 10) peak in the RSM scans (see supplementary Fig. S3).

layer. This fully strained component has a clear effect on the observed MIT, suppressing it as the film thickness reaches values close to the thickness of the fully strained component with an accompanying substantial increase in resistivity at all temperatures. The thicker films, however, display larger transitions with clearer hysteresis in the temperature dependent resistivity between measurements recorded during cooling and heating (Fig. 4). Generally a higher c/a ratio is correlated to a suppression of the transition and the observation of a metallic state at all temperatures [18]. However, our results reveal that the fully strained component displays an insulating state at all temperatures. Thin layers of V_2O_3 have previously been observed to undergo a transition from a metallic to a semiconducting state with decreasing thickness for films which do not display an MIT with temperature [11]. A similar suppression has been observed for films grown by pulsed laser deposition [20, 21], while contradicting results, revealing a suppression of the insulating state with decreasing thickness, have also been observed [4]. It should be noted that these previous studies were performed on films grown with different deposition techniques and substantially higher thicknesses than are discussed here.

The presence of an increased resistivity in ultra-thin V_2O_3 films has been attributed to the presence of a surface dead layer at the interface [22, 23]. This effect arises from the exponential suppression of quasi-particles below the surface of bulk V_2O_3. Although this effect could easily carry over to real systems they would be expected to be obscured by other phenomena [22]. Our results show a clear attenuation and effect on the MIT at the interface as well as a substantial increase in the room temperature resistivity of the metallic state with decreasing thickness. Considering the large difference in the lattice parameters within the fully strained interface layer, compared to bulk, we attribute the properties of the interface layer to arise from the substantially increased strain observed in the interface layer.

In conclusion, we have shown the possibility of growing ultra-thin highly crystalline V_2O_3 layers down to 1 nm thicknesses. Electrical characterization and x-ray diffraction investigations reveal the growth of V_2O_3 thin films on Al_2O_3 (0001) substrates to start with a fully strained epitaxial interface layer where the in-plane lattice parameters of V_2O_3 are matched to the underlying Al_2O_3 substrate. We show that this layer extends ∼4 nm after which the V_2O_3 relaxes to closer to bulk like lattice parameters with an initial high mosaicity that decreases with increasing thickness. Resistivity measurements as a function of temperature show the interface layer to have a substantially higher resistivity at room temperature and attenuated MIT which is regained in the thicker films. The difference in the transport properties of the interface layer compared to the thicker films and bulk V_2O_3 are attributed to the increased strain in the interface layer.

Supplementary material

See supplementary material for further details regarding thin film growth and characterization methods, overview of reciprocal space maps for the sample series and extracted lattice parameters.

Acknowledgments

This work was supported by the University of Iceland Research Fund for Doctoral Students, the University of Iceland Research Fund, the Icelandic Student Innovation Fund and the Icelandic Research Fund (grants 207111 and 174271).

The data that support the findings of this study are available from the corresponding author upon reasonable request.

[1] M. Foex, Comptes rendus hebdomadaires des séances de l'Académie des sciences **223**, 1126 (1946).
[2] D. McWhan and J. Remeika, Physical Review B **2**, 3734 (1970).
[3] F. Giorgianni, J. Sakai, and S. Lupi, Nature Communications **10**, 1159 (2019).
[4] L. Dillemans, T. Smets, R. R. Lieten, M. Menghini, C. Y. Su, and J. P. Locquet, Applied Physics Letters **104**,

071902 (2014).
[5] H. Schuler, S. Klimm, G. Weißmann, C. Renner, and S. Horn, Thin Solid Films **299**, 119 (1997).
[6] J. Sakai, M. Bavencoffe, B. Negulescu, P. Limelette, J. Wolfman, A. Tateyama, and H. Funakubo, Journal of Applied Physics **125**, 115102 (2019).
[7] N. Alyabyeva, J. Sakai, M. Bavencoffe, J. Wolfman, P. Limelette, H. Funakubo, and A. Ruyter, Applied Physics Letters **113**, 241603 (2018).
[8] I. Valmianski, J. G. Ramirez, C. Urban, X. Batlle, and I. K. Schuller, Physical Review B **95**, 155132 (2017).
[9] M. Imada, Journal of the Physical Society of Japan **73**, 1851 (2004).
[10] P. Homm, L. Dillemans, M. Menghini, B. Van Bilzen, P. Bakalov, C.-Y. Su, R. Lieten, M. Houssa, D. Nasr Esfahani, L. Covaci, et al., Applied Physics Letters **107**, 111904 (2015).
[11] Q. Luo, Q. Guo, and E. Wang, Applied physics letters **84**, 2337 (2004).
[12] J. Brockman, M. Samant, K. Roche, and S. Parkin, Applied Physics Letters **101**, 051606 (2012).
[13] B. Allimi, M. Aindow, and S. Alpay, Applied Physics Letters **93**, 112109 (2008).
[14] U. B. Arnalds, J. S. Agustsson, A. S. Ingason, A. K. Eriksson, K. B. Gylfason, J. T. Gudmundsson, and S. Olafsson, Review of Scientific Instruments **78**, 103901 (2007).
[15] National Bureau of Standards (US) Monograph **25**, 108 (1983).
[16] E. B. Thorsteinsson, S. Shayestehaminzadeh, and U. B. Arnalds, Applied Physics Letters **112**, 161902 (2018).
[17] E. B. Thorsteinsson, S. Shayestehaminzadeh, A. S. Ingason, F. Magnus, and U. B. Arnalds, Manuscript. (2020).
[18] J. Sakai, P. Limelette, and H. Funakubo, Applied Physics Letters **107**, 241901 (2015).
[19] H. Schuler, S. Klimm, G. Weissmann, C. Renner, and S. Horn, Thin Solid Films **299**, 119 (1997).
[20] C. Grygiel, C. Simon, B. Mercey, W. Prellier, R. Frésard, and P. Limelette, Applied Physics Letters **91**, 262103 (2007).
[21] S. Yonezawa, Y. Muraoka, Y. Ueda, and Z. Hiroi, Solid State Communications **129**, 245 (2004).
[22] G. Borghi, M. Fabrizio, and E. Tosatti, Physical Review Letters **102**, 066806 (2009), 0901.2706.
[23] F. Rodolakis, B. Mansart, E. Papalazarou, S. Gorovikov, P. Vilmercati, L. Petaccia, A. Goldoni, J. P. Rueff, S. Lupi, P. Metcalf, et al., Physical Review Letters **102**, 066805 (2009).